

IN VIVO CORNEAL CONFOCAL MICROSCOPY: BASIC PRINCIPLES AND APPLICATIONS

SUMMARY

Corneal confocal microscopy is a new, non-invasive imaging method. It provides serial images of a face optical sections through the full-thickness of the living cornea, avoiding artefacts associated with *ex vivo* study. It provides qualitative as well as quantitative analysis of the corneal layers, nerves, and cells. It also allows longitudinal examination of the corneal structure changes over time.

The purpose of this article is to describe the principles and capabilities of the currently available corneal confocal microscopes, and possible applications of this tool.

Key words: confocal microscopy, cornea

Čes. a slov. Oftal., 73, 2017, No. 4, p. 155–160

INTRODUCTION

A confocal microscope was first described by Goldmann in 1940, and later patented in 1957 by M. Minsky (6, 10). Ten years later, M. Petrář and M. Hadravský from the Faculty of Medicine of Charles University in Plzeň patented a confocal microscopy on the basis of a Nipkow scanning disk (23). The first quality optical cross-sections from a strong preparation, specifically brain tissue, were obtained with this instrument (in the professional literature it is known under the title Tandem Scanning Confocal Microscope).

At present, the principle of confocal microscopy is used also for *in vivo* imaging of the surface of the eye, in particular the cornea. The method enables imaging of the individual layers of the cornea in a frontal plane. It is non-invasive and represents a quick method for displaying the cornea in a “natural” (physiological) state, without artefacts caused by the processing of *ex vivo* preparations. It enables qualitative and quantitative assessment of the structure of the individual layers of the cornea – the number of cells, nerve fibres and their morphology, as well as observation of changes over time (2, 6, 8, 10).

In the Czech ophthalmological literature, basic information about the method and the possibilities for its use, primarily in the diagnosis and observation of pathologies of the cornea, has been published by Pirnerová et al. (27). At present a rapid development of this method is taking place, and thus an attendant expansion of the possibilities of its use. The work summarises the current options for instrument equipment and application of this imaging technique.

Principle of confocal microscopy

The resolution capacity of classic optical microscopes is limited by interference phenomena to approx. 0.2 μm , in which this limit is difficult to attain in practice, especially in the case of stronger preparations. The influence of parasitic illumination in particular has an adverse effect. Far more light is reflected from the non-focused planes than from the focused plane. The disruptive blurring of the image by light from the non-focal planes can be got rid of to a considerable extent with the aid of confocal microscopy.

The term confocal (“with the same focus”) indicates an optical system in which the lens and condenser are focused on the same point. In the confocal microscope, the light of the point source is focused on a selected point onto the plane of the preparation, and the light reflected or passed through it is focused onto a point screen, which catches the light incoming from the surrounding area, both from the sides and from locations above and below the focal plane. This screen therefore acts as a spatial filter. Light which does not carry information from the selected point of the preparation is excluded from the formation of the resulting image. The intensity of the light in the image plane decreases very rapidly with the increasing distance

Mahelková G.^{1,2}, Česká Burdová M.¹,
Odehnal M.¹, Dotřelová D.¹

¹Department of Ophthalmology for Children and Adults, 2nd Faculty of Medicine, Charles University and Motol University Hospital

²Institute of Physiology, 2nd Faculty of Medicine, Charles University

Supported by the project (Ministry of Health of the Czech Republic) of conceptual development of research organisation 00064203 and project CZ.2.16/3.1.00/24022.

The authors of the study declare that no conflict of interest exists in the compilation, theme and subsequent publication of this professional communication, and that it is not supported by any pharmaceuticals company.



MUDr. Gabriela Mahelková, Ph.D.
Oční klinika dětí a dospělých 2. LF UK
a FN Motol
V Úvalu 84
150 06 Praha 5 Motol
e-mail: gabriela.mahelkova@fnmotol.cz

from the observed point, and as a result the imaging system has a very low depth of field and a high resolution capacity (15, 24).

In vivo corneal confocal microscopy

In 1985, Lemp et al. published the first confocal images of the cornea in its full thickness (14). As we have already mentioned above, the confocal system has a reduced depth of field in comparison with conventional microscopes, with not only higher quality axial but at the same time also lateral resolution. Clinical corneal confocal microscopes have a typical depth of field from 4 to 26 μm , according to the type of microscope, and a lateral resolution of 1-2 μm . At the same time, the system arranged in this manner is limited by the very small visual field. It thus obtains a larger visual field with the aid of progressive imaging "point by point". This may be theoretically ensured either by movement of the sample in front of a stationary microscope, movement of the microscope above a stationary sample, or sweeping of the beam. Modern in vivo confocal microscopes use the second or third option. Lateral resolution is further limited by the speed of recording the individual pictures (images), because upon recording live objects we cannot entirely exclude the possibility of involuntary movements (breathing, eye movement). The signal produced by the reflected light of the in vivo confocal microscope is typically further detected by an electronic device of the type of a CCD camera. Images are captured with a speed of at minimum 25 images per second (10, 12, 20).

At present we may encounter three types of clinically used in vivo corneal confocal microscopes in the literature:

1. Tandem Scanning confocal microscope – TSCM; Tandem Scanning, Reston, Virginia, USA and Advanced Scanning Corporation, New Orleans, LA, USA; both no longer commercially available.
2. Slit-scanning confocal microscope – SSCM; ConfoScan 4 (ConfoScan 3) Nidek Technologies, Italy; Tomey Corporation, Cambridge, MA, USA and Helmut Hund, Wetzlar, Germany.
3. Heidelberg Retina Tomograph Rostock Corneal Module laser scanning confocal microscope – HRT II or HRT III; Heidelberg Engineering, Heidelberg, Germany (6, 8, 12).

Tandem scanning confocal microscope (TSCM)

TSCM works on the basis of a Nipkow scanning disk, which contains more than 64 000 point openings with a diameter of 20-60 μm (according to type of microscope) arranged in an Archimedean spiral. Each opening has a conjugated opening on the opposite side of the disk. The disk rotates at a speed of 900 revolutions per minute. At each moment light passes through approximately 100 openings. The reflected light passes through a conjugated opening on the other side of the disk. The rotation of the disk thus enables the recording of the entire sample. The ratio of the surface of the disk to the openings determines the quantity of light passing through, which is generally 0.5% - 1% (0.5% for openings of 20 μm). We obtain an image with a relatively low contrast, which may limit the display of small structures (under 5 μm). Furthermore, for compensation of the small quantity of through-passing

light it is necessary to use a strong light source (xenon or mercury arc lamp). This may cause more pronounced dazzling of the patient during examination (6, 12, 20).

Slit scanning confocal microscope (SSCM)

This type of confocal microscope uses an aperture for illumination and observation in the form of a narrow vertical slit. A rapidly oscillating double-sided mirror progressively records confocal images from the illuminating and displaying slit. The slit aperture (300 μm in the case of the type Confoscan 4, NIDEK Technologies) enables a greater quantity of penetrating light than in the case of TSCM, which increases the brightness and contrast of the observed field. Thanks to this the observed structures are displayed more clearly, sharply and with more details. The higher penetration of light also enables a reduction of the intensity of lighting (12-V halogen lamp), which guarantees greater comfort for the patient. The increased brightness and contrast in SSCM is partially attained at the expense of the increased depth of acuity, which in the case of Confoscan 3 and Confoscan 4 is approximately 26 μm . The use of a slit also means that the microscope is genuinely confocal only in the axis perpendicular to the height of the slit. The forward step between the images can be set from 1 μm , during one recording it is possible to obtain up to 350 images. Upon a set step of 5 μm we therefore record the cornea in its entire thickness twice in one cycle (6, 16, 20).

Laser scanning confocal microscope Heidelberg Retina Tomograph Rostock Corneal Module (LSCM)

An example of LSCM is the Heidelberg Retina Tomograph Rostock Corneal Module (HRT II or HRT III), which uses a coherent red light with a wavelength of 670 nm from a helium neon laser source. This concerns a class 1 laser, which according to the definition does not represent any danger for the eye. Nevertheless, according to the instructions of the manufacturer, in order to ensure the safety of the examiner and the examined patient, the length of an individual examination should not exceed 3 000 s (50 min).

The laser beam is projected progressively above each point of the examined area. For recording of the image, the laser beam must be deflected in two mutually perpendicular directions. This is attained by two recording mirrors: a resonance scanner records the beam horizontally and a galvanometric scanner records this line vertically, thus creating an image of the visual field. The recording of the reflected light is ensured by the same two mirrors. The reflected light is deflected onto a detector (diode), subsequently the signal is digitised and an image is created. According to the data from the manufacturer, the lateral resolution of this microscope is 1 μm and the depth of acuity 4 μm . In manual mode it is possible to obtain optical cross-sections through the entire thickness of the cornea, with the aid of automatic mode, however, it is possible to obtain only cross-sections within the range of 80 μm of thickness (6, 25).

Images from confocal microscope

The quality of images generally depends on two main factors: contrast and resolution. Resolution depends on the

numerical aperture of the lens, reflectivity of the observed structures and the wavelength of the illuminating light.

All of the above-stated types of instruments can be used to obtain images on the level of microstructure of the cornea. Morphological changes are visible in the structure of the epithelial and endothelial cells, the nucleus of keratocytes, and in certain cases also the body of keratocytes and their tips, the nerve fibres and heterogeneous elements – fibres of mould and other microorganisms. Another advantage is the possibility of a quantitative evaluation of the displayed structures under normal circumstances also in the cases of pathologies or following surgical procedures on the cornea. The quality of the captured structures may however differ significantly depending on the type of used instrument and also on the experience of the examiner (5, 16, 20).

All the aforementioned corneal confocal microscopes require a certain type of contact with the cornea upon examination. In the case of TSCM and SSCM, optical contact is mediated by a viscous gel applied to the lens of the instrument. In the case of LSCM, a special addition (cover) is fitted onto the lens, which flattens the cornea during examination. In all cases we obtain images of the individual layers of the cornea in the frontal plane. Images obtained by LSCM have a higher contrast than SSCM and TSCM. In addition to this, in the case of SSCM contrast also declines in the direction toward the periphery of the images. It is also necessary to be aware that the size of the objects on the obtained images can be directly compared only on images obtained from the same type of microscope, and upon the use of the same lighting intensity (6, 29).

Image of individual layers of cornea upon examination by corneal confocal microscope

The cornea is a specialised transparent tissue which is at the same time the main refractive part of the optical system of the eye. Its capability to transmit light is thanks to the precise organisation of the individual layers and components of the extracellular matrix, correct hydration and avascularity.

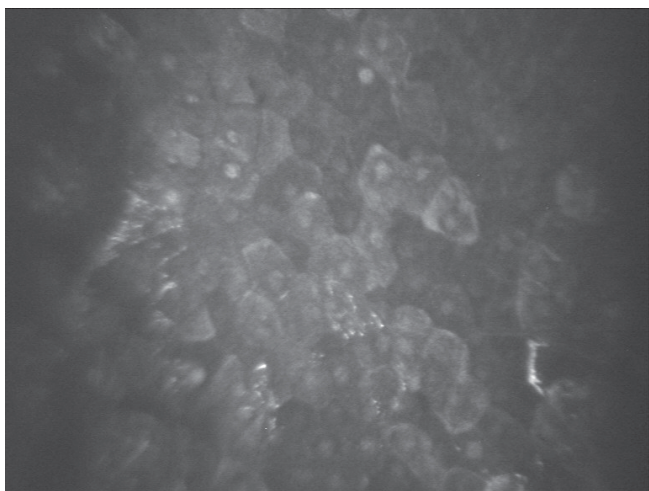


Fig. 1 Epithelial layer. Surface epithelial cells (SSCM; Confoscan 3, NIDEK Technologies)

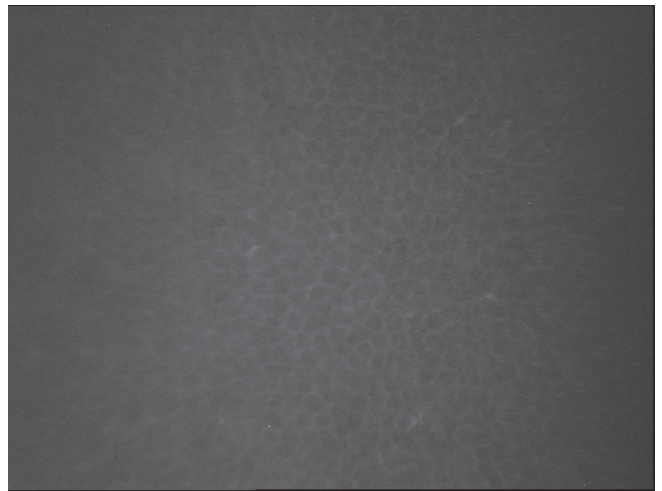


Fig. 2 Epithelial layer. Basal epithelial cells (SSCM; Confoscan 3, NIDEK Technologies)

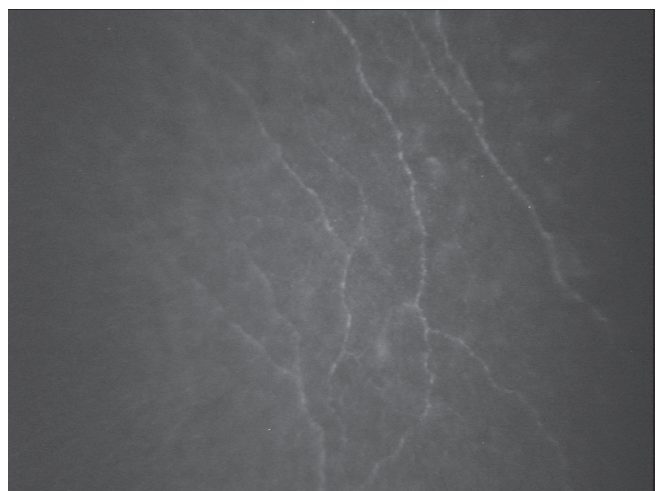


Fig. 3 Fibres of subepithelial nerve plexus (SSCM; Confoscan 3, NIDEK Technologies)

We differentiate between 5 layers in the cornea: the corneal epithelium (formed by 6 layers of progressively flattening cells), the Bowman's membrane, the stroma, the Descemet's membrane and the endothelium. 90% of the corneal tissue is made up of the stroma. It is formed precisely by arranged lamellas of collagen fibres and proteoglycans, which are synthesised by the stromal cells – keratocytes. The endothelium is formed by one layer of cells. It plays a fundamental role in maintaining correct hydration of the cornea (7).

Confocal microscopy of the cornea enables imaging of the individual layers of the cornea in vivo.

In the corneal epithelium we can progressively display the layers of 3 types of cells: flat surface cells (fig. 1), polygonal intermediary cells and the layer of cylindrical basal cells (fig. 2). The normal values of cellular density and cell size in the individual layers differ markedly in different individuals.

It is not usually possible to display the details of the acellular structures of the basal membrane of the epithelium and the Bowman's membrane. However, in healthy corneas the

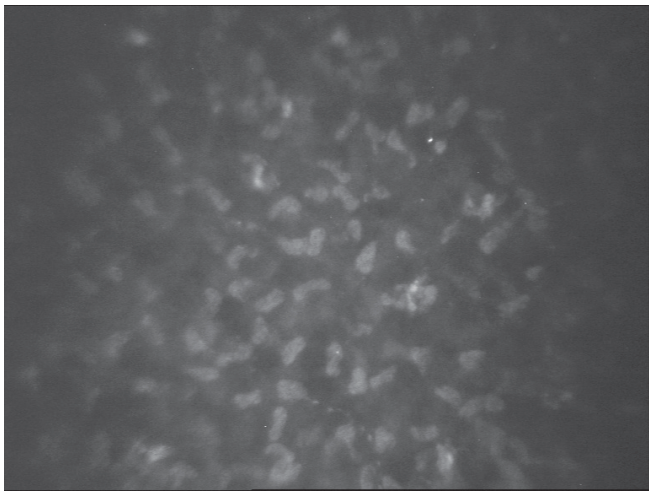


Fig. 4 Stroma. Anterior stroma with visible nuclei of keratocytes (SSCM; Confoscan 3, NIDEK Technologies)

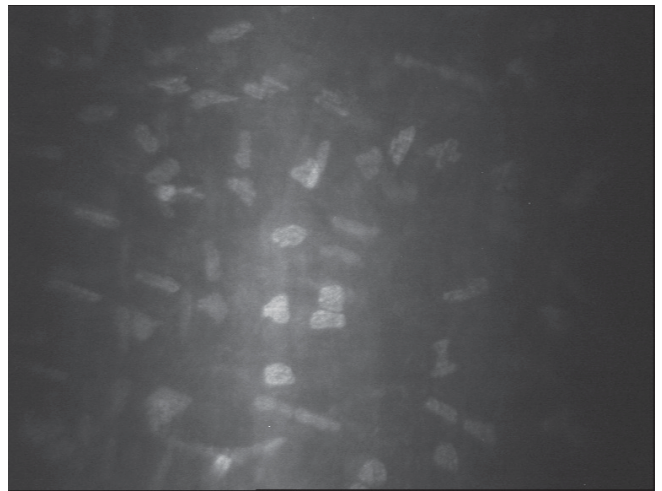


Fig. 5 Stroma. Anterior stroma with visible nuclei of keratocytes (SSCM; Confoscan 3, NIDEK Technologies)

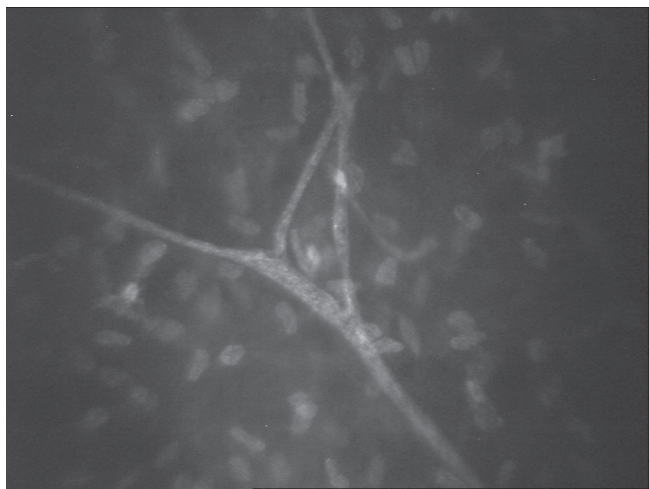


Fig. 6 Stroma. Stromal nerve – Y branching (SSCM; Confoscan 3, NIDEK Technologies)

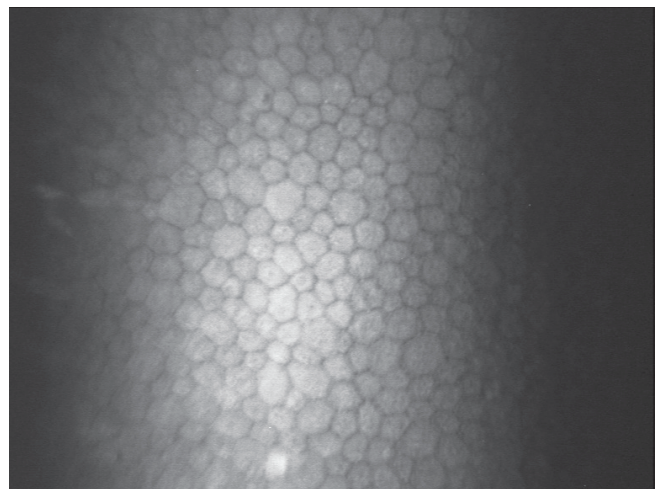


Fig. 7 Endothelial layer. Hexagonal endothelial cells (SSCM; Confoscan 3, NIDEK Technologies)

subbasal nerve plexus, located between the layer of the basal epithelial cells and the anterior layers of the Bowman's membrane, as well as the subepithelial plexus, located beneath the Bowman's membrane, can be easily distinguished (fig. 3).

The corneal stroma represents 80-90% of the total volume of the corneal tissue. Here we can differentiate between the cellular, acellular and neurosensoric components. The cellular component comprises above all keratocytes, which form approximately 5% of the total volume of the stroma. The acellular component (90-95% of the stroma) consists of precisely arranged collagen lamellas and other components of the extracellular matrix. The third component consists of the above-described nerve plexus and isolated stromal nerve fibres. In the image of the confocal microscope we typically find irregular reflective oval bodies, which represent the nuclei of the keratocytes, and are surrounded by the virtually transparent (dark grey or black) acellular matrix. In the absence of pathological processes in the stroma, the components of the extracellular matrix are not displayed due to their virtually perfect transparency, which is a con-

dition for the normal functioning of the cornea. The average density of keratocytes is highest in the anterior stroma (fig. 4), decreases in the direction of the layers of the central stroma, and subsequently increases slightly again in the posterior stroma (fig. 5) (2). In addition, nerve fibres located in the deep stromal plexus are displayed in the stroma, primarily in its surface layers. The nerve fibres here are three to five times thicker than the fibres of the subbasal and subepithelial plexus, and we frequently also identify typical branching in an Y shape (fig. 6). Nerve fibres are not usually found in the posterior layers of the stroma.

In healthy corneas the Descemet's membrane, similarly to the Bowman's membrane, cannot be displayed on a confocal microscope. However, its pathological changes upon certain corneal pathologies can be displayed, such as posterior corneal dystrophy or changes in primary congenital glaucoma.

The innermost layer consists of the single-layer endothelium. It is displayed as a layer of hexagonal or polygonal regularly arranged cells (fig. 7). The density of the endothelial cells is highest upon birth, and progressively decreases during the

course of life. The Descemet's membrane and the endothelium are not supplied by nerves in humans (3, 6, 8, 9, 10, 17).

Comparison of results acquired with the aid of various types of instruments

Upon a comparison of instruments working on the principle of white light and laser, no fundamental differences were found in displaying the structures of a healthy and pathological cornea. It appears that for the study of changes of epithelial cells it is possible to obtain better imaging with the aid of LSCM, whereas by contrast for the study of changes of the endothelium, the use of SSCM (Confoscan 3, NIDEK Technology) appears to be more advantageous. Upon examination with the aid of LSCM, direct contact of the instrument (lens or its cover) with the cornea takes place, and this may lead to the generation of certain artefacts. A typical finding upon examination by LSCM is frequently observed folds in the region of the Descemet's membrane, which may imitate the findings e.g. upon keratoconus or postoperatively in the area of the disc following keratoplasty. Significant differences have also been found in an evaluation of the density of endothelial cells using both systems. The numbers of endothelial cells upon evaluation with the aid of LSCM are significantly higher than the results obtained with the aid of Confoscan 3 and specular microscope SP1000, Topcon (5, 9, 20).

Recently, a large amount of attention has been devoted also to changes of the subbasal nerve plexus in various systemic pathologies such as diabetes mellitus, rheumatological pathologies and neurological pathologies, e.g. Parkinson's disease, amyotrophic lateral sclerosis, idiopathic small-fibre polyneuropathy (1, 11, 18, 19, 21, 31, 32). An SSCM and LSCM instrument was used primarily for imaging nerve

fibres. The evaluated parameters usually include the total number of (main) nerve fibres, the total length of the nerve fibres, number of branchings and tortuosity of nerve fibres (30). The absolute values converted to mm² may differ according to the used instrument. The length and number of nerve fibres (19, 26) was evaluated as a highly reproducible parameter. In general the value of the total length of fibres in studies conducted on instruments of the SSCM and TSCM type is lower than upon the use of LSCM, whereas conversely the total number of fibres is higher (28). Potentially interesting, but to date without a fully resolved system of evaluation, is the parameter of tortuosity (4, 13). At present, mainly the use of the LSCM system is becoming more widespread, since it has higher resolution and enables better imaging of the corneal epithelium and the anterior stroma, including the nerve plexus. The latest instruments also contain automatic software for evaluation of the images and e.g. the possibility of reconstructing 3D images (19, 28).

CONCLUSION

In the last ten years there has been a pronounced expansion of the use of in vivo confocal microscopy of the cornea. The advantages of this method include its non-invasiveness, and thus also its usability not only for the diagnosis of changes in the structure of the cornea, but also for observing the development of these changes over time and the effect of treatment. Upon an evaluation of the results of various studies, it is necessary to keep in mind that it is not possible to compare directly results obtained upon examination on different types of corneal confocal microscopes (5, 29). In future it shall be necessary to further standardise the methodology and the manner of evaluating the results of examination.

LITERATURE

1. **Alhatem, A., Cavalcanti, B., Hamrah, P.:** In vivo confocal microscopy in dry eye disease and related conditions. *Semin Ophthalmol*, 2012; 27: 138–148.
2. **Alzubaidi, R., Sharif, M.S., Qahwaji, R., et al.:** In vivo confocal microscopic corneal images in health and disease with an emphasis on extracting features and visual signatures for corneal diseases: a review study. *Br J Ophthalmol*, 2016; 100: 41–55.
3. **Chiou, A.G., Kaufman, S.C., Kaufman, H.E., et al.:** Clinical corneal confocal microscopy. *Surv Ophthalmol*, 2006; 51: 482–500.
4. **Edwards, K., Pritchard, N., Vagenas, D., et al.:** Standardizing corneal nerve fibre length for nerve tortuosity increases its association with measures of diabetic neuropathy. *Diabet Med*, 2014; 31: 1205–1209.
5. **Erie, E.A., McLaren, J.W., Kittleson, K.M., et al.:** Corneal subbasal nerve density: a comparison of two confocal microscopes. *Eye Contact Lens*, 2008; 34: 322–325.
6. **Erie, J.C., McLaren, J.W., Patel, S.V.:** Confocal microscopy in ophthalmology. *Am J Ophthalmol*, 2009; 148: 639–646.
7. **Forrester, J, Dick, A., McMenamin, P., et al.(Eds):** *The Eye: Basic Science in Practice*. 2002, s. 178–187.
8. **Guthoff, R.F., Zhivov, A., Stachs, O.:** In vivo confocal microscopy, an inner vision of the cornea – a major review. *Clin Experiment Ophthalmol*, 2009; 37: 100–117.
9. **Hollingsworth, J., Perez-Gomez, I., Mutalib, H.A., et al.:** A population study of the normal cornea using an in vivo, slit-scanning confocal microscope. *Optom Vis Sci*, 2001; 78: 706–711.
10. **Jalbert, I., Stapleton, F., Papas, E., et al.:** In vivo confocal microscopy of the human cornea. *Br J Ophthalmol*, 2003; 87: 225–236.
11. **Jiang, M.S., Yuan, Y., Gu, Z.X., et al.:** Corneal confocal microscopy for assessment of diabetic peripheral neuropathy: a meta-analysis. *Br J Ophthalmol*, 2016; 100: 9–14.
12. **Kaufman, S.C., Kaufman, H.E.:** How has confocal microscopy helped us in refractive surgery? *Curr Opin Ophthalmol*, 2006; 17: 380–388.
13. **Lagali, N., Poletti, E., Patel, D.V., et al.:** Focused Tortuosity Definitions Based on Expert Clinical Assessment of Corneal Subbasal Nerves. *Invest Ophthalmol Vis Sci*, 2015; 56: 5102–5109.
14. **Lemp, M.A., Dilly, P.N., Boyde, A.:** Tandem-scanning (confocal) microscopy of the full-thickness cornea. *Cornea*, 1985; 4: 205–209.
15. **Lovblom, L.E., Halpern, E.M., Wu, T., et al.:** In vivo corneal confocal microscopy and prediction of future incident neuropathy in type 1 diabetes: a preliminary longitudinal analysis. *Can J Diabetes*, 2015; 39: 390–397.
16. **Masters, B.R., Bohnke, M.:** Confocal microscopy of the human cornea in vivo. *Int Ophthalmol*, 2001; 23: 199–206.
17. **Mastropasqua, L., Nubile, N. (Eds):**

- Confocal Microscopy of the Cornea. Thorofare, NJ USA, SLACK Incorporated, 2002, s.7–16.
18. **Misra, S.L., Craig, J.P., Patel, D.V., et al.:** In Vivo Confocal Microscopy of Corneal Nerves: An Ocular Biomarker for Peripheral and Cardiac Autonomic Neuropathy in Type 1 Diabetes Mellitus. *Invest Ophthalmol Vis Sci*, 2015; 56: 5060–5065.
 19. **Papanas, N., Ziegler, D.:** Corneal confocal microscopy: Recent progress in the evaluation of diabetic neuropathy. *J Diabetes Investig*, 2015; 6: 381–389.
 20. **Patel, D.V., McGhee, C.N.:** Contemporary in vivo confocal microscopy of the living human cornea using white light and laser scanning techniques: a major review. *Clin Experiment Ophthalmol*, 2007; 35: 71–88.
 21. **Patel, D.V., McGhee, C.N.:** In vivo confocal microscopy of human corneal nerves in health, in ocular and systemic disease, and following corneal surgery: a review. *Br J Ophthalmol*, 2009; 93: 853–860.
 22. **Patel, D.V., Tavakoli, M., Craig, J.P., et al.:** Corneal sensitivity and slit scanning in vivo confocal microscopy of the subbasal nerve plexus of the normal central and peripheral human cornea. *Cornea*, 2009; 28: 735–740.
 23. **Petran, M., Hadravsky, M., Egger, M., et al.:** Tandem-scanning reflected-light microscope. *J Opt Soc Am* 1968; 58: 661–664.
 24. **Petroll, W.M., Cavanagh, H.D., Jester, J.V.:** Confocal microscopy. In Krachmer, J., Mannis, M., Holland, E.(Eds), *Cornea: Fundamentals, Diagnosis and Management*. MOSBY, Elsevier, 2011, s. 205–211.
 25. **Petroll, W.M., Robertson, D.M.:** In Vivo Confocal Microscopy of the Cornea: New Developments in Image Acquisition, Reconstruction, and Analysis Using the HRT-Rostock Corneal Module. *Ocul Surf*, 2015; 13: 187–203.
 26. **Petropoulos, I.N., Manzoor, T., Morgan, P., et al.:** Repeatability of in vivo corneal confocal microscopy to quantify corneal nerve morphology. *Cornea* 2013; 32: e83-89.
 27. **Pirnerová L, Horácková M, Vlková E, Hlinomazová Z, Trnková V, Strmenová E.:** Využití konfokální mikroskopie rohovky v klinické praxi. *Čes a Slov Oftalmol*, 2010; 66(6): 239–47.
 28. **Prakasam, R.K., Winter, K., Schwiede, M., et al.:** Characteristic quantities of corneal epithelial structures in confocal laser scanning microscopic volume data sets. *Cornea* 2013; 32: 636–643.
 29. **Szaflik, J.P.:** Comparison of in vivo confocal microscopy of human cornea by white light scanning slit and laser scanning systems. *Cornea*, 2007; 26: 438–445.
 30. **Tavakoli, M., Ferdousi, M., Petropoulos, I.N., et al.:** Normative values for corneal nerve morphology assessed using corneal confocal microscopy: a multinational normative data set. *Diabetes Care* 2015; 38: 838–843.
 31. **Tavakoli, M., Petropoulos, I.N., Malik, R.A.:** Corneal confocal microscopy to assess diabetic neuropathy: an eye on the foot. *J Diabetes Sci Technol*, 2013; 7: 1179–1189.
 32. **Wang, E.F., Misra, S.L., Patel, D.V.:** In Vivo Confocal Microscopy of the Human Cornea in the Assessment of Peripheral Neuropathy and Systemic Diseases. *Biomed Res Int*, 2015; 95: 1081.